

A Thorough Analysis of Two Different Pre-Lithiation Techniques for Silicon/Carbon Negative Electrodes in Lithium Ion Batteries

Gerrit Michael Overhoff,^[a] Roman Nölle,^[b] Vassilios Siozios,^[b] Martin Winter,^{*[a, b]} and Tobias Placke^{*[b]}

Silicon (Si) is one of the most promising candidates for application as high-capacity negative electrode (anode) material in lithium ion batteries (LIBs) due to its high specific capacity. However, evoked by huge volume changes upon (de)lithiation, several issues lead to a rather poor electrochemical performance of Si-based LIB cells. The Coulombic efficiency (C_{Eff}) during the first cycle(s), especially when using nano-sized Si, is relatively low, due to the formation of the solid electrolyte interphase (SEI). Pre-lithiation approaches can increase the C_{Eff} by compensating active lithium losses during the first cycle(s). Here, we evaluate the beneficial impact of pre-lithiated Si/C electrodes for their application in NCM111 | | Si/C cells by

comparing two approaches, *i.e.*, electrochemical pre-lithiation and pre-lithiation by direct contact to Li metal foil. The SEI composition and surface morphology of pre-lithiated Si/C electrodes as well as the impact of reducing active Li losses on individual electrode potentials over cycling are revealed. For long-term cycling, both pre-lithiation techniques lead to a distinct improvement of the overall capacity as well as the C_{Eff} for the first 40 cycles due to i) the pre-formed SEI and ii) a Li reservoir within the anode. Depletion of the active Li from NCM111 is significantly reduced and we can confirm that both pre-lithiation techniques improve the cycling performance of NCM111 | | Si/C cells in an almost equal manner.

1. Introduction

Among the various Li storage materials,^[1] silicon (Si) is considered as one of the most promising materials to be incorporated within negative electrodes (anodes) to increase the energy density of current lithium ion batteries (LIBs). Si has higher capacities than other Li storage metals, however, the incorporation of significant amounts of Si (> 10%) in commercial LIB cells is still hampered due to the poor cycle life of such Si-based cells.^[2] This is mainly related to the huge volume expansion of Si upon lithiation up to 280%, causing severe structural instability of the active material itself (*i.e.*, cracking and pulverization of Si particles) as well as of the whole composite electrode (*i.e.*, contact loss to the conductive network and current collector).^[3] Typically, these issues can be readily addressed by downsizing the Li storage metal particle size to the nanoscale range (*e.g.*, nanoparticles (NPs)), which

are able to accommodate such huge volume changes without cracking. Si-NPs generally exhibit an improved cycle life compared to micron-sized particles.^[4] However, the huge increase of the specific surface area of NPs comes along with a severe handicap, namely higher reactivity, or instance with the electrolyte leading to an increased active lithium loss (ALL)^[5] related to the formation of the solid electrolyte interphase (SEI).^[6] Therefore, Si-NPs typically suffer from a poor Coulombic efficiency (C_{Eff}) during the first and ongoing cycles, which drastically reduces the reversible capacity and, thus, energy density of LIB full-cells with limited active lithium content.^[7] Pre-treatment or “pre-lithiation” is a common strategy to address the issues of nano-sized materials by reducing ALL *via* formation of the SEI layer prior to cell assembly or by *in situ* pre-lithiation during cell operation.^[8] Besides compensation of ALL within the first charge/discharge cycle(s), there are also approaches to load a reservoir of active Li into LIB cells by partial lithiation of the anode *via* pre-lithiation to address ongoing ALL during cycling,^[9] which was shown to be highly beneficial for an improved cycling stability of Si-based full-cells. The Li reservoir can compensate continuous ALL as a result of ongoing SEI breakage and re-formation during cycling, which typically results in severe capacity fading.^[10] However, the creation of a reservoir needs to be adjusted with a high accuracy, as over-lithiation of the anode would lead to an excess of lithium, resulting in Li metal plating on the top of the anode surface (if the N:P ratio is not adjusted accordingly) and, subsequently, leading to safety hazards during operation. Therefore, a suitable balance between high energy and high cycle life needs to be found for pre-lithiated Si/C full-cells.

[a] G. M. Overhoff, Prof. Dr. M. Winter
Helmholtz Institute Münster
IEK-12, Forschungszentrum Jülich GmbH
Corrensstr. 46, 48149 Münster, Germany
E-mail: m.winter@fz-juelich.de

[b] Dr. R. Nölle, Dr. V. Siozios, Prof. Dr. M. Winter, Dr. T. Placke
University of Münster
MEET Battery Research Center, Institute of Physical Chemistry
Corrensstr. 46, 48149 Münster, Germany
E-mail: tobias.placke@uni-muenster.de

 Supporting information for this article is available on the WWW under
<https://doi.org/10.1002/batt.202100024>

 © 2021 The Authors. *Batteries & Supercaps* published by Wiley-VCH GmbH.
This is an open access article under the terms of the Creative Commons Attribution License, which permits use, distribution and reproduction in any medium, provided the original work is properly cited.

There are several pre-lithiation techniques described in literature, e.g., pre-lithiation by contacting the anode to Li metal (e.g., in form of foil or powder) in presence of electrolyte or electrochemical pre-lithiation by simply “pre-cycling” or “pre-formation” of the anode within a half-cell setup^[7b] using a Li metal counter electrode (CE) being the most prominent ones for laboratory purposes.^[8a,b,11] Whereas both pre-lithiation methods have proven to be very effective to address the issues of initial and ongoing ALL in LIB cells, a thorough comparison of the effectiveness between both techniques is missing so far. Since different research studies typically vary in parameters including the active material (e.g., type of active material, particle size, etc.), composite electrode (composition, mass loading, etc.) the cell configuration (half-cell vs. full-cell setup)^[7b] or the pre-lithiation conditions itself (e.g., amount of pre-lithiation, pre-lithiation speed, electrolyte, etc.), a fair comparison and conclusion on which technique might be more effective is not possible. *Saito et al.* were the first to directly compare electrochemical pre-lithiation and “contact pre-lithiation” (*via* Li metal foil) of anodes based on Si–NPs, concluding contact pre-lithiation to be more effective than electrochemical pre-lithiation in terms of depth and homogeneity of pre-lithiation.^[12] However, in their study only half-cells with a Li metal CE^[7b] and, therefore, an unlimited amount of active Li were used for electrochemical analysis. Furthermore, higher amounts of Li were added to the Si negative electrodes by the contact pre-lithiation approach, which was proven to be related to the faster pre-lithiation going along with pulverization of the Si–NPs.^[12] If Si-based anodes are coupled with a typical cathode material (e.g., $\text{Li}[\text{Ni}_x\text{Co}_y\text{Mn}_z]\text{O}_2$ (NCM)^[13]) within an LIB full-cell, such high degrees of lithiation of the Si anode prior to cell assembly might result in Li metal plating upon charging, as mentioned above. Recently, *Bärmann et al.* reported on the challenges to achieve a high homogeneity of pre-lithiation on the macroscopic (electrode) and microscopic (particle) levels for silicon/carbon electrodes pre-lithiated by Li metal.^[11g]

In this study, both contact pre-lithiation *via* Li metal foil and electrochemical pre-lithiation of silicon/amorphous carbon (Si/C) composite electrodes, which exhibit a reversible capacity of $\approx 1080 \text{ mAh g}^{-1}$, are systematically evaluated and compared. To enable a fair comparison of both techniques, the pre-lithiation degree of the Si/C electrodes was carefully controlled and equalized. The electrode morphology and the SEI formed at the Si/C electrode surface were examined by scanning electron microscopy (SEM) and X-ray photoelectron spectroscopy (XPS), respectively. Finally, the pre-lithiated Si/C composite electrodes were evaluated in $\text{LiNi}_{1/3}\text{Co}_{1/3}\text{Mn}_{1/3}\text{O}_2$ (NCM111) || Si/C full-cells to demonstrate the effectiveness for compensating the poor C_{eff} and ALL of Si-based full-cells *via* the two pre-lithiation techniques.

Experimental Section

Electrode Preparation

Si/C composite electrodes were prepared by wet coating of an aqueous electrode paste with a composition of 55 wt.% amorphous (soft) carbon (D50: 11.9 μm ; *SGL carbon*) and 30 wt.% Si–NPs (180 nm, *Wacker Chemie AG*) as active materials, 10 wt.% binder (polyacrylic acid, *Sigma Aldrich*, average $M_v \approx 450,000$) and 5 wt.% conductive agent (carbon black, *Super C65, Imerys Graphite & Carbon*). The mixture was dispersed at 10,000 rpm for 90 min by a Dispermat LC30 by VMA. The paste was cast onto dendritic copper foil (thickness = 20 μm , *Carl Schlenk AG*) using a lab-scale doctor blade technique. The electrode sheets were dried at 80 °C for 1 h before cutting out circular disks (Ø12 mm), which were dried again at 110 °C for 24 h under reduced pressure of $1 \cdot 10^{-3}$ mbar. The Si/C electrodes had a dry film thickness of ≈ 30 – $32 \mu\text{m}$, an average mass loading of $\approx 1.44 \text{ mg cm}^{-2}$ and an areal capacity of 1.32 mAh cm^{-2} , which was calculated based on the active material's practical specific capacity of $1,080 \text{ mAh g}^{-1}$. For LIB full-cells, commercial NCM111-based electrodes (*Custom Cells Itzehoe GmbH*) were applied as the positive electrode (cathode). Circular disks (Ø12 mm) were punched and dried at 110 °C for 24 h under reduced pressure of $1 \cdot 10^{-3}$ mbar. The average mass loading was $\approx 8.26 \text{ mg cm}^{-2}$ with an active material content of 86%, delivering a specific capacity of 1.03 mAh cm^{-2} in the potential range of 3.0–4.3 V vs. $\text{Li}|\text{Li}^+$ (practical specific capacity of the active material: $\approx 145 \text{ mAh g}^{-1}$). Electrode storage and all cell (dis)assembly steps were carried out in an argon-filled glovebox (*MBraun*) with oxygen and water contents below 0.1 ppm.

Pre-Lithiation of Silicon/Carbon Composite Electrodes

Pre-lithiation via direct contact to Li metal (Method 1): The pre-lithiation was conducted in Swagelok-type cells by pressing Si/C electrodes with a constant pressure onto high-purity Li metal foil (thickness $\approx 500 \mu\text{m}$, battery grade, *Albemarle Corporation*) without usage of a separator. To enable sufficient contact between both electrodes, Li metal was wetted with 60 μL of electrolyte (1 M LiPF_6 in EC/DEC 3:7 (w/w) + 2 wt.% VC, battery grade, *UBE*). The pressing time was varied between 10 and 60 minutes.

Electrochemical pre-lithiation (Method 2): In case of electrochemical pre-lithiation, Swagelok-type Si/C || Li metal cells (half-cell setup, three-electrode configuration)^[7b] were assembled using Si/C electrodes as working electrode (WE), Li metal foil as CE and reference electrode (RE) and a polyolefin separator (FS2190, 3 layers, Ø13 mm and Ø10 mm for RE, *Freudenberg Performance Materials*) wetted with 120 μL (80 μL for RE) electrolyte (1 M LiPF_6 in EC/DEC 3:7 (w/w) + 2 wt.% VC). The Si/C electrodes were lithiated in constant current mode to a potential of 0.02 V vs. $\text{Li}|\text{Li}^+$ with a specific current of 2,000 mA g^{-1} (referring to the active material of Si/C electrodes) and 100 mA g^{-1} for 15 min and 5 h, respectively, followed by an OCP step (10 min). Afterwards, the cells were disassembled, and the Si/C electrodes transferred into a new cell without washing.

Electrochemical Investigations of Pre-Lithiated Si/C Electrodes

Three-electrode cells were prepared like the procedure described above. The long-term cycling stability was investigated by constant current-constant voltage cycling on a *MacCor 4000 battery tester* at 20 °C. The Si/C || Li metal cells (half-cell setup) were cycled in a WE potential range of 0.02–1.50 V vs. $\text{Li}|\text{Li}^+$ with a specific current of 300 mA g^{-1} (referring to the electrode's active material: 1 C

corresponds to 1080 mA g^{-1}), while three formation cycles were performed at 200 mA g^{-1} . For NCM111||Si/C full-cells, a specific current of 45 mA g^{-1} was applied (referring to the cathode active material: 1 C corresponds to 145 mA g^{-1}), while three formation cycles were performed at 30 mA g^{-1} , and the cells were cycled in a cell voltage range of $3.0\text{--}4.3 \text{ V}$. After charging of the Si/C electrode, in both cell setups a constant potential/voltage step was performed until the specific current dropped below 0.05 C. The specific capacities and the C-rate shown for NCM111||Si/C full-cells refer to the active material content of the NCM111 electrode and the electrodes were matched with a N:P capacity balancing ratio of $\approx 1.28:1.00$.

X-Ray Photoelectron Spectroscopy and Scanning Electron Microscopy Investigations of Pre-Lithiated Electrodes

The pre-lithiated Si/C electrodes were harvested from the cells, rinsed with $150 \mu\text{L}$ dimethyl carbonate (DMC; battery grade), *i.e.*, twice for X-ray photoelectron spectroscopy (XPS) and six times for scanning electron microscopy (SEM) measurements, to remove LiPF_6 salt residues from the surface. Afterwards, they were dried under reduced pressure ($1\text{--}10^{-3} \text{ mbar}$) for 10 min and transferred to the devices avoiding exposure to ambient air. SEM investigations were performed using a *Carl Zeiss AURIGA CrossBeam* workstation with a *Schottky* field emission gun. Images were obtained with a secondary electron detector at an acceleration voltage of 5 kV and a working distance of 6 mm. For XPS investigations, the samples were analyzed with a XPS device (*Axis Ultra DLD, Kratos*) by applying a monochromatic Al K α source ($h\nu=1486.6 \text{ eV}$) with a 10 mA filament current and a 12 kV filament voltage source. To compensate charging of the samples, a charge neutralizer was used. The measurements were performed at a 0° angle of emission, a pass energy of 20 eV and a pressure of $1\text{--}10^{-7} \text{ Pa}$ in the analysis chamber. Subsequent fitting was performed with *CasaXPS*, where the C 1s C–H/C–C peak (binding energy (BE)=284.5 eV) was used as an internal reference to calibrate the BE of the recorded spectra. Three spots of each sample were measured to verify reproducibility.

2. Results and Discussion

2.1. Study of Lithiation Degree of Si/C Electrodes in Dependency on the Time of Pre-Lithiation via Li Metal

Finding the ideal lithiation degree *via* pre-lithiation is crucial in order to accurately adjust the amount of Li for compensation of ALL during the first cycles, without provoking detrimental Li metal plating.^[11g] To get deeper insights into the lithiation capacity of the electrodes after pre-lithiation, Si/C electrodes were pre-lithiated using Li metal for different times, *i.e.*, 10, 30 and 60 min. Afterwards, the pre-lithiated electrodes were electrochemically lithiated (charged) in Si/C||Li metal cells

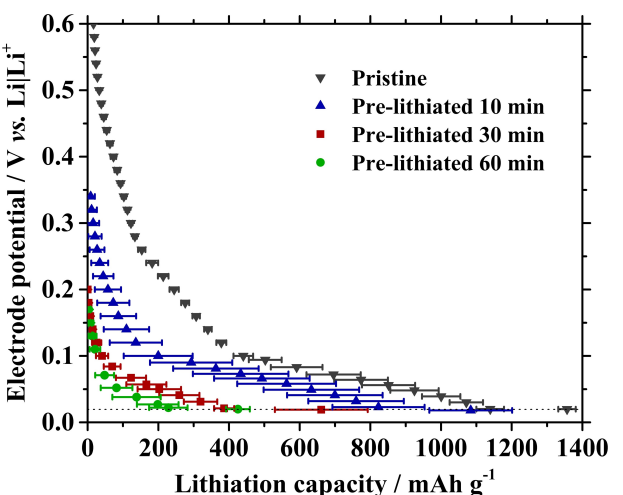


Figure 1. Si/C electrode potential vs. initial lithiation capacity of pristine and pre-lithiated Si/C electrodes (*via* Li metal at 10, 30 and 60 min). The Si/C||Li metal cells (half-cell setup) were lithiated at 200 mA g^{-1} to a WE potential of 20 mV vs. $\text{Li}|\text{Li}^+$ followed by a constant potential step until the specific current dropped below 50 mA g^{-1} .

(half-cell setup) and compared with pristine ones (Figure 1 and Table 1).

The Si/C pristine electrode possesses the highest lithiation capacity (1397 mAh g^{-1}). For the pre-lithiated Si/C electrodes, the initial lithiation capacity gradually decreases with increasing pre-lithiation time to 425 mAh g^{-1} after 60 min of pre-lithiation *via* Li metal, which means that $\approx 70\%$ of the electrodes' lithiation capacity is already obtained during the pre-lithiation step. After 10 min contact pre-lithiation, the electrodes exhibit two sloping potential plateaus (*i.e.*, $0.26\text{--}0.1 \text{ V}$ vs. $\text{Li}|\text{Li}^+$ and below 0.1 V vs. $\text{Li}|\text{Li}^+$), while the electrodes after pre-lithiation for 30 and 60 min only show a single sloping plateau during lithiation ($<0.1 \text{ V}$ vs. $\text{Li}|\text{Li}^+$). In comparison, pristine (non-pre-lithiated) Si–NP electrodes exhibit also both plateaus in the same potential regions during lithiation (Figure S1, *Supporting Information*).^[3b] Furthermore, the lithiation of pristine (non-pre-lithiated) amorphous carbon electrodes starts at $\approx 0.9 \text{ V}$ vs. $\text{Li}|\text{Li}^+$ and proceeds continuously over the whole potential range to 0.02 V vs. $\text{Li}|\text{Li}^+$, which is in agreement with literature (Figure S1).^[14] Hence, after 10 min of pre-lithiation the major part of the lithiation capacity contributes to SEI formation or lithiation of amorphous carbon, as both plateaus corresponding to lithiation of silicon are still visible in the potential profile (Figure 1). For the two other pre-lithiation times (30 and 60 minutes), only the second lithiation plateau for silicon (below 0.1 V vs. $\text{Li}|\text{Li}^+$) can be detected during the first charge.

Table 1. Initial lithiation capacities, open circuit potentials (OCPs) before electrochemical lithiation and 1st cycle Coulombic efficiency of pristine and pre-lithiated Si/C electrodes (*via* Li metal at different times) when lithiated in a Si/C||Li metal cell (half-cell setup).

	Pristine	Pre-lithiated <i>via</i> Li metal for 10 min	30 min	60 min
Initial lithiation capacity [mAh g^{-1}]	$1,397 \pm 45$	$1,084 \pm 117$	661 ± 131	425 ± 34
OCP before lithiation [V] vs. $\text{Li} \text{Li}^+$	3.07 ± 0.15	0.41 ± 0.08	0.25 ± 0.03	0.20 ± 0.01
Coulombic efficiency 1 st cycle [%]	83.3 ± 1.1	112.4 ± 17.0	182.8 ± 36.1	296.3 ± 32.3

This observation suggests that besides lithiation of amorphous carbon also lithiation of silicon occurred partially during the pre-lithiation step (Figure 1). In comparison, the pristine Si–NP electrodes show an additional charge capacity above 0.25 V vs. Li|Li⁺, due to electrolyte decomposition and the formation of the protective SEI layer (Figure S1).^[15]

In addition to the initial lithiation capacity discussed above, the open circuit potential (OCP) and the 1st cycle Coulombic efficiency (C_{Eff}) of the pre-lithiated and pristine Si/C electrodes are depicted in Table 1. Increasing the pre-lithiation time results in a lower OCP of the Si/C composite electrode, relating to a higher lithiation degree of the active material, which agrees with the decreasing initial lithiation capacity of the pre-lithiated electrodes (Figure 1). Furthermore, an OCP shift to higher potentials is noticed for all electrodes after pre-lithiation and cell reassembly, which gradates over time. This effect is most likely attributed to a “self-discharge” mechanism of a reactive lithium silicide phase formed at low potentials with the electrolyte and ongoing SEI formation as described by Key *et al.* for Si electrodes.^[16] Recently, Bärmann *et al.* also reported on the OCP shift and on the impact of the crystalline Li₁₅Si₄ phase vs. the amorphous Si phase on the self-discharge mechanism.^[17] The occurrence of parasitic reactions for Si/C composite electrodes was also observed by Kalaga *et al.* during potentiostatic aging studies, leading to capacity loss of the cell.^[18] The pristine Si/C electrodes possess a first cycle C_{Eff} of $\approx 83.3\%$, indicating that a significant amount of active Li is consumed for SEI formation. In an LIB full-cell setup, where the amount of active Li is limited, this Li consumption would result in a reduced active Li content, and therefore, a lower overall reversible capacity. After pre-lithiation of the Si/C electrode, the C_{Eff} of the first cycle can be enhanced to $\approx 112.4\%$ and $\approx 296.3\%$ after 10 and 60 min, respectively. Even though a clear trend can be observed, the high error ranges (Table 1) also show the drawback of pre-lithiation *via* Li metal foil, *i.e.*, difficulties in terms of a high reproducibility. In particular, it is very challenging to precisely adjust the degree of pre-lithiation as Li metal foil is used in large excess and minor variations at the Li metal|Si/C interface as well as at the Si/C|electrolyte interface can have a significant impact on the degree of pre-lithiation within a specific time. Therefore, pre-lithiation by using Li metal powder is widely pursued in research studies, allowing a much more precise adjustment of the degree of pre-lithiation by choosing the proper amount of Li metal. However, safe handling of Li metal powder is challenging and must be performed very carefully (in dry atmosphere) to avoid safety issues.^[8a]

The C_{Eff} values $>100\%$ illustrate that more Li can be extracted from the Si/C electrode in the first cycle after pre-lithiation, meaning that a Li reservoir is present in the Si/C electrode, which can improve the cycling performance of LIB full-cells by compensating ongoing ALL.^[9]

To further investigate the impact of the pre-lithiation time on the cycling performance of the Si/C electrodes, long-term charge/discharge cycling was performed for pristine and pre-lithiated (10/30/60 min *via* Li metal) electrodes in Si/C||Li metal cells (Figure S2). All cells show a very similar behavior in

terms of de-lithiation capacity, C_{Eff} and capacity retention within the standard deviation, indicating that neither the pre-lithiation setup nor the pre-lithiation time impairs the performance of the Si/C electrodes within Si/C||Li metal cells. In summary, the different contact pre-lithiation times were evaluated to find the “right pre-lithiation degree” to allow for a suitable comparison with the electrochemically pre-lithiated Si/C electrodes. It should be noted that the capacity fading in Figure S2 is caused by degradation effects such as cracking or pulverization of particles or contact losses of constituents of the composite electrode, rather than active lithium losses due to SEI breakage/re-formation, because of an enormous Li excess provided by the Li metal CE.

2.2. Electrochemical Pre-Lithiation at Different Specific Currents

Electrochemical pre-lithiation is a well-established laboratory approach and is widely used in research studies because of its simple setup and high accuracy by easily adjusting the applied current and voltage/potential range.^[8a,11a,19] For a proper comparison between electrochemical pre-lithiation and contact pre-lithiation *via* Li metal, it is important to adjust the pre-lithiation degree to the same level. The results discussed above showed that the 1st cycle C_{Eff} after 10 min of contact pre-lithiation is close to $\approx 100\%$, which is why it is chosen as appropriate reference. The overall capacity C_{Li} (=amount of Li transferred to the Si/C electrode) during the 10-min pre-lithiation was calculated from the capacities for active Li (C_{active}) (lithiation of the active materials) and inactive Li (C_{inactive}) [immobilized in the SEI, Eq. (1)]:

$$C_{\text{Li}} = C_{\text{active}} + C_{\text{inactive}} \quad (1)$$

C_{active} corresponds to the de-lithiation capacity of the Si/C anode immediately after 10 min of pre-lithiation ($= 306 \text{ mAh g}^{-1}$) and the irreversible capacity (C_{inactive}) can be calculated by the difference between the initial lithiation capacity ($C_{\text{Li},1^{\text{st}} \text{ cycle}}$) and initial de-lithiation capacity ($C_{\text{de-Li},1^{\text{st}} \text{ cycle}}$) of the pristine Si/C electrode [Eq. (2)].

$$C_{\text{inactive}} = C_{\text{Li},1^{\text{st}} \text{ cycle}} - C_{\text{de-Li},1^{\text{st}} \text{ cycle}} = 233 \text{ mAh g}^{-1} \quad (2)$$

which results in a capacity for C_{Li} of 539 mAh g^{-1} . However, for the calculation of C_{inactive} it has to be assumed that the active Li losses during SEI formation by contact pre-lithiation using Li metal are comparable to those of a pristine electrode during its initial cycle (related to the irreversible capacity). However, there are different factors such as Si particle cracking and electronic contact losses contributing to the difference between $C_{\text{Li},1^{\text{st}} \text{ cycle}}$ and $C_{\text{de-Li},1^{\text{st}} \text{ cycle}}$ which might have an impact on the irreversible capacity. Thus, a capacity of 500 mAh g^{-1} was chosen as target value (C_{Li}) for electrochemical pre-lithiation.

Si/C electrodes were electrochemically pre-lithiated at two specific currents of $2,000 \text{ mA g}^{-1}$ and 100 mA g^{-1} for 15 min and 5 h, respectively, so that the same amount of electric charge is

transferred (Figure 2). Figure 2a shows the potential as function of the pre-lithiation time and Figure 2b the potential as function of the specific lithiation capacity. The high specific current for the latter approach results in the formation of high overpotentials and almost immediately to a potential drop below 0.5 V vs. Li|Li⁺ (Figure 2a, b). The occurrence of overpotentials can be confirmed by taking a closer look at the OCP after the pre-lithiation step. The potential of electrodes pre-lithiated at 2,000 mA g⁻¹ increases to ≥ 160 mV within 10 min after pre-lithiation, whereas for the ones pre-lithiated at low specific current, only an increase of ≈ 20 mV can be observed within 10 min. High specific currents during pre-lithiation cause huge stress and may damage the Si/C electrode due to a rapid volume expansion. In addition, for specific currents higher than 2000 mA g⁻¹, the potential dropped below 0 V vs. Li|Li⁺ (not shown here).

2.3. Comparison of Pre-Lithiated Si/C Electrodes via Electrochemical and Contact Approaches

The initial lithiation capacity and the OCP of pre-lithiated Si/C electrodes are shown in Table 2. The mean values for the initial lithiation capacity and the OCP of the Si/C electrodes are similar for all three cases (considering the error ranges), meaning that the amount of transferred Li to the Si/C electrode during 10 min of pre-lithiation via Li metal was precise enough to obtain electrochemically pre-lithiated electrodes with the same lithiation degree. However, the standard deviation of the

electrodes pre-lithiated using Li metal is higher, as mentioned above. Minor variations of the electrode properties (porosity, surface roughness, etc.) as well as of the pre-lithiation setup (Li metal surface, wetting of the electrodes, pressure during pre-lithiation) can have a significant impact on the pre-lithiation degree during pre-lithiation via Li metal and, therefore, result in higher deviations of the initial lithiation capacity.

Differential capacity (dQ/dV) vs. potential profiles of the 1st cycle (after pre-lithiation) are shown for different cells as a function of the Si/C electrode potential in Figure 3. In all cases, a broad peak is visible at < 0.15 V vs. Li|Li⁺, representing the lithiation of crystalline Si–NPs (c-Si) to form the amorphous silicide (a -Li_xSi) phases.^[3b,20] These results are in good agreement with previous investigations where only minor lithiation of the Si–NPs during pre-lithiation was shown, so that most of the Si particles remain as c-Si. De-lithiation results in two peaks at 0.30 V and 0.45 V vs. Li|Li⁺, confirming de-lithiation of a -Li_xSi to form a -Si.^[3b] As the de-lithiation of the amorphous carbon material occurs over the whole potential range, no distinct peaks are visible. However, during the beginning of lithiation (highlighted in the insets), differences between pre-lithiated and pristine electrodes are detected. The differential capacity of pristine electrodes increases from 0.90 V vs. Li|Li⁺, having one broad plateau down to 0.30 V vs. Li|Li⁺ and an additional peak at 0.25 V vs. Li|Li⁺ (Figure 3a). The latter peak is most likely related to lithiation of small amounts of a -Si structures (two characteristic peaks at 0.10 V and 0.25 V vs. Li|Li⁺) with the first one being overlaid by the peak below 0.10 V vs. Li|Li⁺ for lithiation of c-Si.^[3b] In addition, the differential capacity increase

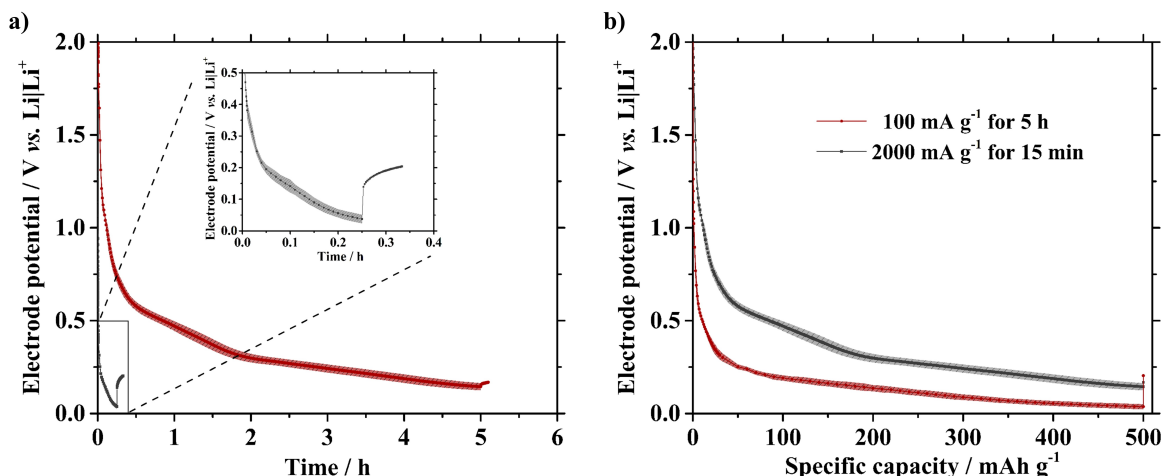


Figure 2. Potential profiles of Si/C electrodes (a) vs. time and (b) vs. specific capacity in a Si/C | | Li metal cell (half-cell setup, three-electrode configuration) during electrochemical pre-lithiation (from OCP) at (i) 2,000 mA g⁻¹ for 15 min and (ii) 100 mA g⁻¹ for 5 h followed by an OCP step (10 min).

Table 2. Initial lithiation capacities and open circuit potentials (OCPs) of pre-lithiated Si/C electrodes using electrochemical and contact approaches, when lithiated in a Si/C | | Li metal cell (half-cell setup).

	Pre-lithiation by Li metal	Electrochemical pre-lithiation	
	10 min	5 h at 100 mA g ⁻¹	15 min at 2,000 mA g ⁻¹
Initial lithiation capacity [mAh g ⁻¹]	1,084 \pm 117	1,081 \pm 59	1,064 \pm 70
OCP before lithiation [V] vs. Li Li ⁺	0.41 \pm 0.08	0.38 \pm 0.08	0.37 \pm 0.05

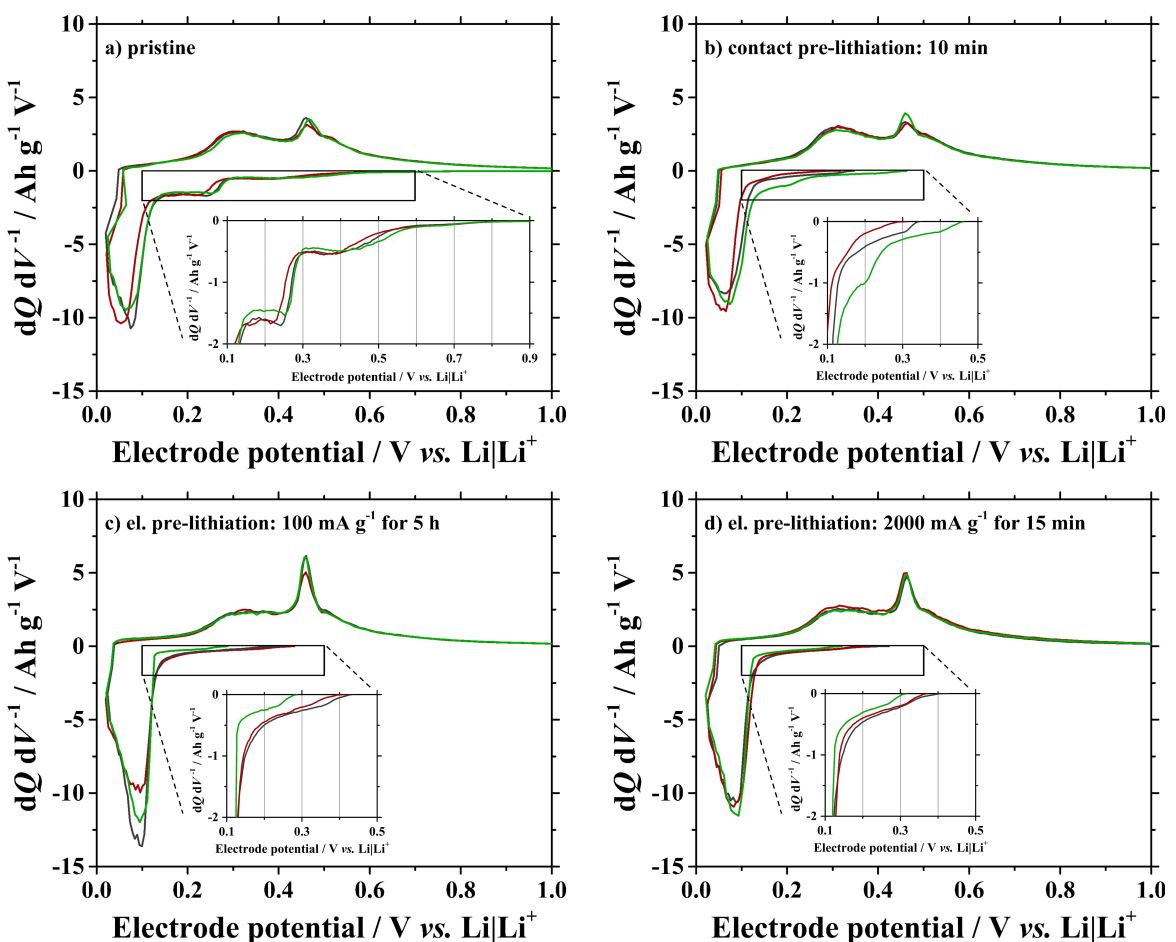


Figure 3. Differential capacity (dQ/dV) vs. potential diagrams as function of the Si/C electrode potential in the 1st cycle of a Si/C || Li metal cell (half-cell setup, three-electrode configuration): a) pristine electrodes, b) electrodes pre-lithiated via Li metal (10 min), c) electrochemically pre-lithiated electrodes at 100 mA g^{-1} for 5 h and d) electrochemically pre-lithiated electrodes at 2000 mA g^{-1} for 15 min. The insets highlight the beginning of lithiation. The different colors refer to three different cells for each pre-lithiation method.

at higher potentials is induced by decomposition of the electrolyte solvents as well as of the additive VC or the conducting salt LiPF₆ to form the SEI.^[21] The lithiation of the amorphous carbon occurs consistent over the whole potential range as well.^[14] In contrast, the pre-lithiated electrodes show less differential capacity increase (Figure 3b-d), indicating an already formed protective SEI layer and partial lithiation of the active material during pre-lithiation. Furthermore, the lower the OCP at the beginning of the cycling procedure, the less increase of differential capacity can be observed for the individual cells prior to the dominant lithiation peak of c-Si.

2.4. Investigation of the SEI Formed During Pre-Lithiation by Means of XPS

For analysis of the surface of Si/C electrodes and the SEI formed during pre-lithiation, XPS measurements were performed after the pre-lithiation steps and were compared to pristine electrodes (Figure 4). In the F 1s spectra, a distinct peak at a binding energy (BE) 684.7 eV is observed for the three pre-lithiated electrodes, which can be assigned to the presence of LiF.^[10c,22]

Noticeably, the intensity of this peak for the Si/C electrode pre-lithiated at 100 mA g^{-1} for 5 h is slightly lower, thus, the SEI formed at the surface of the electrode exhibits less LiF. A second peak at ≈ 687.0 eV, which corresponds to decomposition products of the conductive salt LiPF₆ (e.g., Li_xPO_yF_z) and is often detected after electrochemically cycling investigations,^[10c] was not present yet for none of the pre-lithiated electrodes. The O 1s spectrum of the pristine electrode displays a dominant peak at 533.5 eV, which is attributed to C–O and Si–O bounds.^[23] These signals result mainly from oxide layers at the surface of the Si–NPs and from functional groups of the binder.^[24] For the pre-lithiated electrodes, the main peak is located at 531.4 eV (C=O), which can be attributed to the presence of lithium alkyl-carbonates and/or Li₂CO₃.^[25] The peak at 533.5 eV is at most present as a small shoulder, thus, a SEI layer seems to cover the surface of the electrodes, as the information depth of XPS is ≈ 10 nm. In the spectrum of the pre-lithiated electrode by Li metal, an additional peak is present at ≈ 528 eV, which is related to small quantities of the inorganic species Li₂O formed in the SEI layer.^[22b,25a,26]

In the C 1s spectra, a major peak at 284.5 eV (C–C, C–H) is present for the pre-lithiated electrodes, which is attributed to

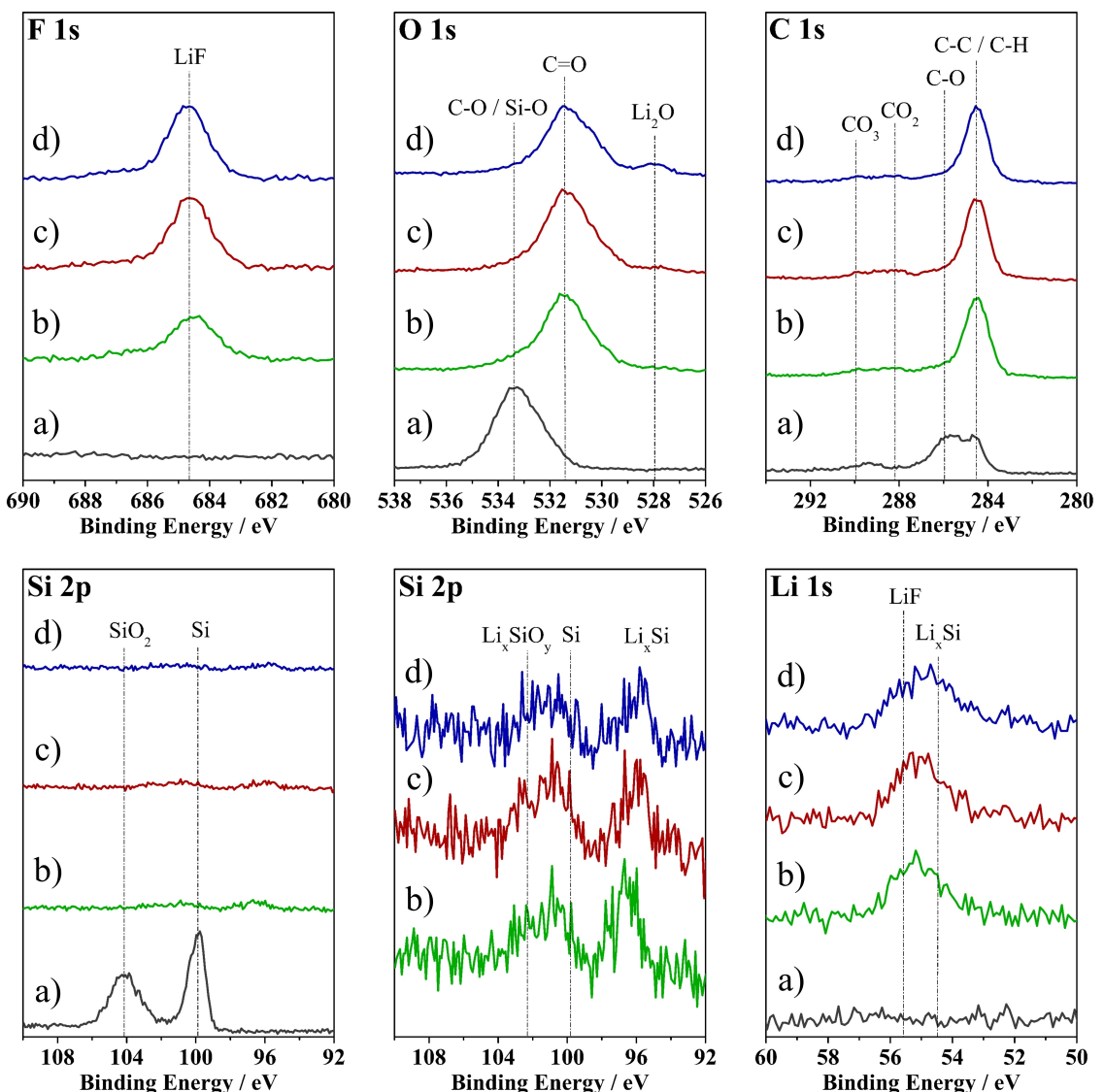


Figure 4. XPS core spectra (F 1s, O 1s, C 1s, Si 2p, Li 1s) of the surface of the Si/C electrodes: a) pristine electrode, b, c) after electrochemical pre-lithiation at (b) 100 mAg^{-1} for 5 h and at (c) 2000 mAg^{-1} for 15 min, d) after pre-lithiation via Li metal for 10 min.

alkane species incorporated in the SEI resulting from decomposition products of the organic electrolyte.^[22b] The spectrum of the pristine Si/C electrode exhibits a broad peak in this BE region, which is related to C–C, C–H and C–O environments arising from the PAA binder.^[24b,26,27] At BEs of 288.2 eV and 289.8 eV, small broad peaks are visible for the pre-lithiated electrodes, indicating the presence of O=C–O functional groups and carbonate species.^[25b,c,28] This is in good agreement with results from the O 1s spectra, where also C=O species were found.

The Si 2p spectrum of the pristine electrode shows a distinct peak at 99.6 eV with a small shoulder to higher BEs, which is related to bulk Si ($2p_{3/2}$ and $2p_{1/2}$ due to spin-orbit coupling).^[10c,28,29] Another peak is present at \approx 104 eV, corresponding to the attendance of SiO_2 at the surface of the pristine electrode and is usually found when the electrode was exposed to air during the preparation.^[21c,28,30] Both peaks can be

attributed to Si-NPs positioned at the top surface layer of the composite electrode. For the pre-lithiated electrodes, these major peaks are not visible anymore, proving that a SEI covers the electrodes surface after pre-lithiation. However, when taking a closer look at the spectra of the pre-lithiated electrodes, small peaks with a very small signal-to-noise ratio can be observed. The first one, at \approx 100–102 eV could arise from Li_xSiO_y species, as reported in literature.^[28,31] The second peak at \approx 96.5 eV is even stronger shifted to lower BEs than that of bulk Si due to a more negatively charged Si. This could indicate the presence of a Li-containing environment, though in literature the phase shift to lower BEs is not reported to be so pronounced in case of lithiated Si species.^[21c,28] However, the presence of peaks in the Si 2p spectra for the pre-lithiated electrodes show that the SEI layer formed at the surface of the electrode after pre-lithiation is either not very thick (< 10 nm) so that electrons emitted from Si atoms can be detected, or it

has a high inhomogeneity, *i.e.*, spots where the Si–NPs are exposed to the surface of the electrode.

In the Li 1s spectrum, a broad peak at ≈ 55.0 eV is present for the pre-lithiated electrodes, which can be assigned to the presence of LiF, which is in good agreement with the findings of the F 1s spectra. Additionally, Li_xSi has been reported to be indicated by a peak at ≈ 54.5 eV, which supports the assumption of an Li_xSi peak in the Si 2p spectra.^[22a]

2.5. Surface Morphology of Pristine and Pre-Lithiated Electrodes

For the analysis of the surface morphology of pre-lithiated and pristine Si/C electrodes, SEM measurements were performed (Figure 5). The purpose of this analysis was to evaluate, whether the pre-lithiation techniques lead to a significant damage of the electrode (due to the volume changes) in comparison to the pristine electrodes. Spherical particles are visible at the surface of all different electrodes, which are related the amorphous carbon with a diameter of up to $\approx 15 \mu\text{m}$. The whole electrode surfaces as well as the carbon particles are covered with a mixture of Si–NPs and carbon black (Figure S3). Several cracks are visible at the surface of the

pristine electrode (Figure 5a), arising from evaporation of the solvent after wet-coating of the electrodes. In contrast, pre-lithiated electrodes show no obvious or only minor cracks at the surface, as these cracks are most likely covered by the formed SEI layer and/or reduced as the electrodes underwent swelling due to lithiation of the active material. The Si/C electrode that has been pre-lithiated for the shortest time (10 minutes) still shows few surface cracks (Figure 5b), while the electrochemically pre-lithiated electrodes (Figure 5c, d) show almost no surface cracks, which is most likely related to surface layer (SEI) formation. Overall, the images of the electrodes of the different pre-lithiation techniques are very similar, not showing any damage caused, *e.g.*, by pre-lithiation *via* direct contact to the Li metal. However, it must be kept in mind that the SEM analysis is limited, as it is nearly impossible to observe the same electrode position in the pristine state and after pre-lithiation. In addition, it should be considered that the pressure during pre-lithiation *via* Li metal or within the electrochemical cells might also have an impact on the electrode surface appearance.

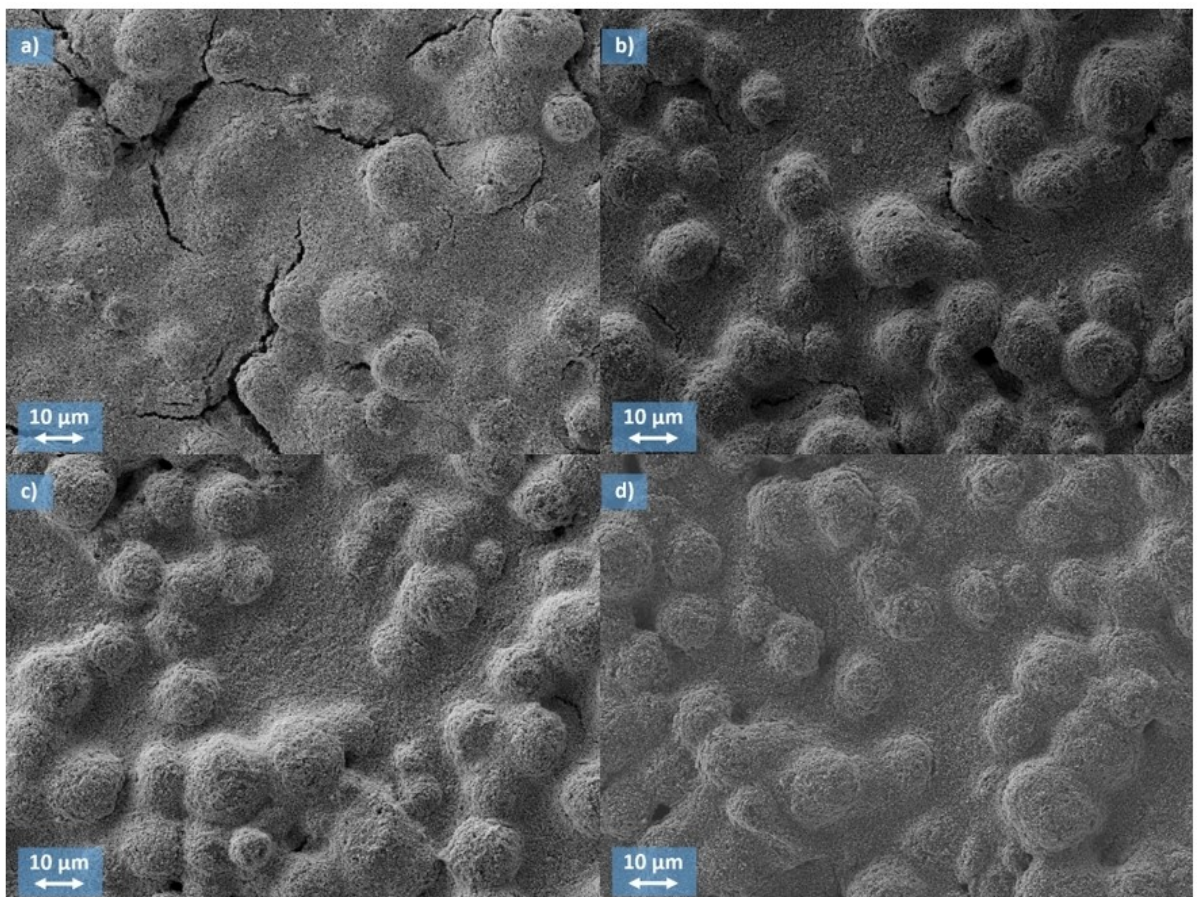


Figure 5. SEM surface analysis of the a) pristine Si/C electrode and b-d) pre-lithiated electrodes: b) pre-lithiated *via* Li metal for 10 min, c) electrochemically pre-lithiated at 100 mAg^{-1} for 5 h, and d) electrochemically pre-lithiated at 2000 mAg^{-1} for 15 min.

2.6. Impact of Pre-Lithiation on the Cycling Performance in NCM111||Si/C Full Cells

The long-term cycling performance of electrochemically and *via* Li metal pre-lithiated Si/C electrodes was conducted in NCM111||Si/C full-cells. The additional Li content from pre-lithiation has to be taken into account when determining the N:P ratio,^[32] as the implementation of a Li reservoir within the negative electrode may lead to Li metal plating due to a capacity-oversized Si/C electrode.^[9a] Therefore, the pristine and pre-lithiated Si/C electrodes were each overbalanced by a N:P ratio of 1.28:1. The cathode active material NCM111 also demonstrates a stable cycling performance and high reproducibility in NCM111||Li metal cells (Figure S4).

In Figure 6, the specific discharge capacity and the C_{Eff} of pre-lithiated and pristine Si/C electrodes in full-cells are shown. The first cycle discharge capacity is increased to $>140 \text{ mAh g}^{-1}$ after pre-lithiation independent of the pre-lithiation technique, in contrast to $\approx 125 \text{ mAh g}^{-1}$ for full-cells using pristine Si/C electrodes. Similarly, the C_{Eff} increases from $\approx 69\%$ to 83% for all pre-lithiated cells. The pre-formed SEI as well as the already partially lithiated active materials (Si, C) can compensate for ALL, resulting in a higher amount of active Li and, therefore, higher capacity and C_{Eff} , respectively. However, the C_{Eff} is not only affected by processes occurring at the anode, but also by kinetic limitations at the cathode during the first cycle which are also visible for NCM111||Li metal cells (half-cell setup; Figure S4), and are not influenced by pre-lithiation.^[33] Notably, pre-lithiation does not only significantly improve the discharge capacity in the first cycle, but also results in an enhanced C_{Eff}

for almost 50 cycles compared to the full-cells using pristine Si/C electrodes (inlet in Figure 6). Only the cells employing electrochemically pre-lithiated Si/C electrodes at $2,000 \text{ mA g}^{-1}$ overlap with the pristine ones for several cycles in regards of their standard deviation. Chevrier *et al.* explained this beneficial effect through the presence of a Li reservoir within the negative electrode compensating for continuous ALL due to SEI breakage and re-formation during cycling.^[9a]

To analyze the impact of pre-lithiation on the individual electrode potentials over cycling, these are presented for selected cycles in Figure 7. When the end-of-charge (EOC) at 4.3 V is reached during the first cycle (Figure 7a), the cathode potential of the full-cell using pristine Si/C anodes is already at higher potentials (4.38 V vs. Li|Li⁺) compared to the cells using pre-lithiated Si/C electrodes, meaning that more active Li is extracted out of the cathode. This is also proven by an increased charge capacity when reaching the EOC. At the end-of-discharge (EODC) at 3.0 V, the cathodes' potential profiles of the pre-lithiated cells all drop rapidly (*i.e.*, showing a strong polarization) $<3.6 \text{ V}$ vs. Li|Li⁺ and indicate that the amount of Li is completely restored (reduced by the amount of irreversible capacity due to kinetic limitations).^[34] The full-cell with the pristine Si/C electrode does not show a potential drop for the positive electrode, but instead the negative electrode potential increases to $\approx 0.8 \text{ V}$ vs. Li|Li⁺ during discharge, which is significantly higher than the pre-lithiated electrodes. For the full-cell using the pristine Si/C electrode, the active Li amount is almost completely extracted out of the anode, but it is not sufficient to completely charge the cathode due to parasitic Li-consuming reactions (SEI formation), while the pre-lithiated

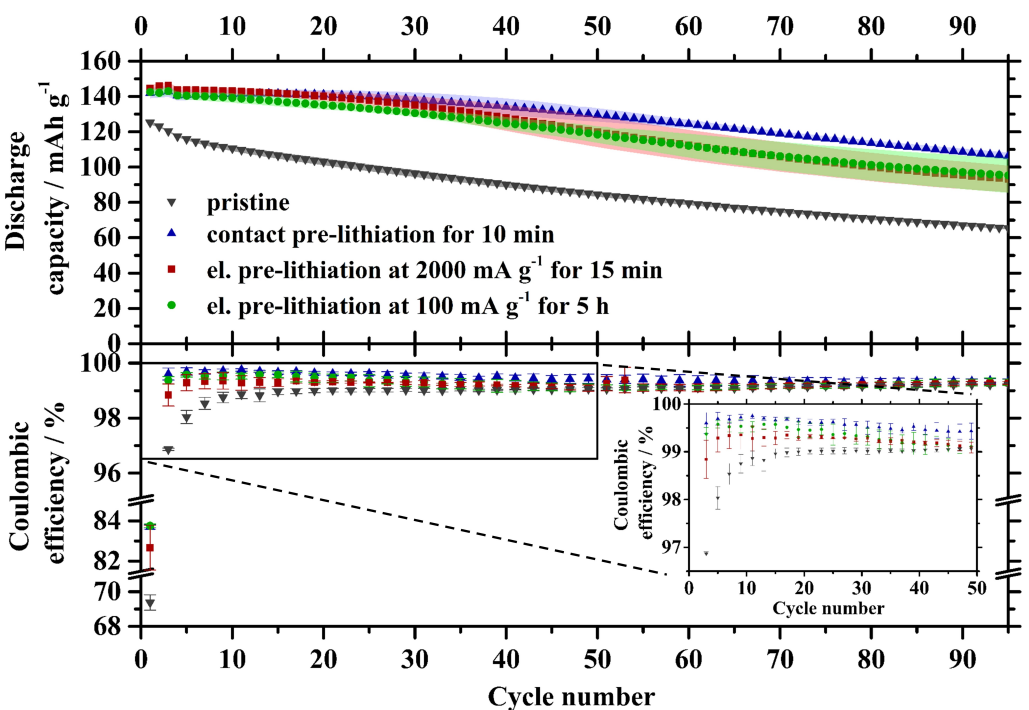


Figure 6. Specific discharge capacities and Coulombic efficiencies of NCM111||Si/C cells (full-cell setup, three-electrode configuration; cell voltage range: 3.0–4.3 V) using pristine, electrochemically and *via* Li metal pre-lithiated Si/C electrodes.

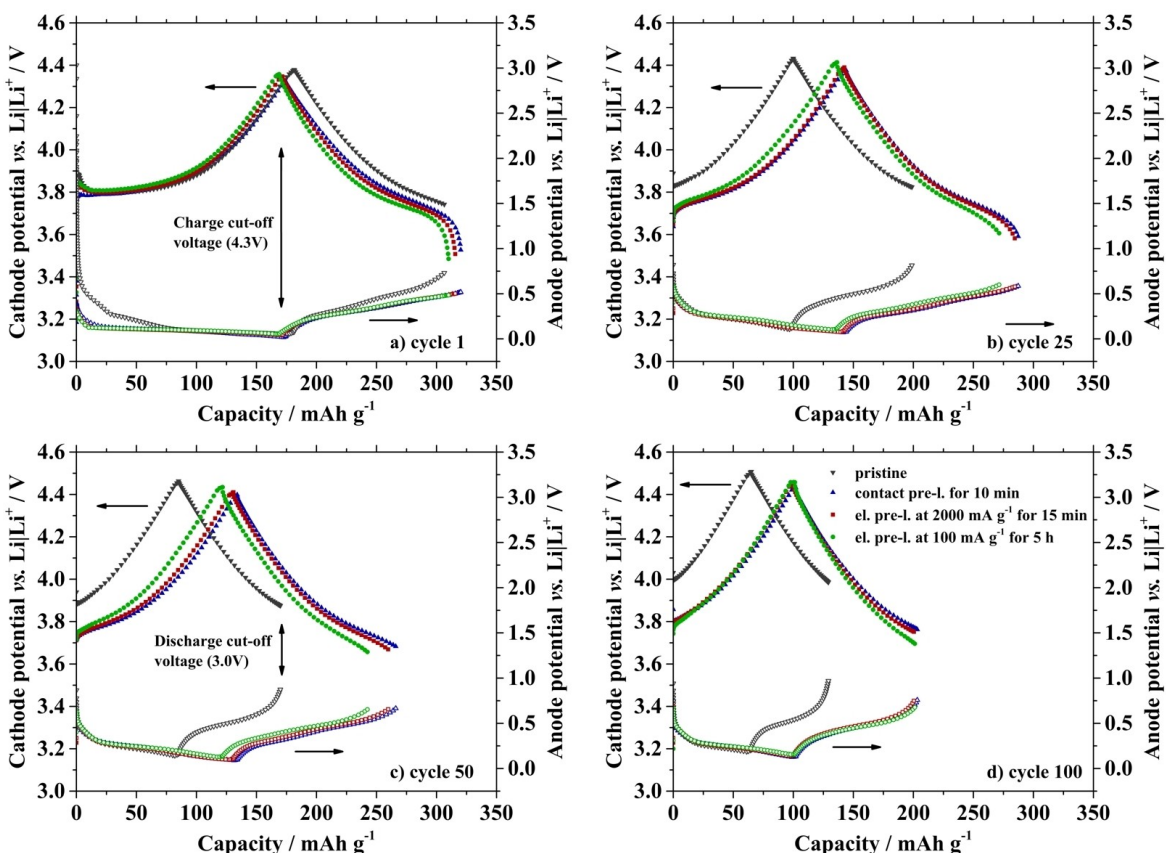


Figure 7. Positive and negative electrode potentials of NCM111 || Si/C cells (full-cell setup, three-electrode configuration; cell voltage range: 3.0–4.3 V) in dependence of the specific capacity for the a) 1st, b) 25th, c) 50th, and d) 100th cycle using pristine and pre-lithiated Si/C electrodes.

cells still obtain a Li reservoir in the negative electrode at the EODC. After 25 cycles, the cells using the pristine Si/C electrode lost 30% of their initial capacity due to a lack of active Li, while the Li reservoir of the cells using pre-lithiated Si/C electrodes buffer on-going ALL (Figure 7b), so that the capacity stays nearly constant (Figure 6). In the potential profiles for the 50th and 100th cycle, the cathodes' potential drop for the pre-lithiated cells cannot be observed anymore, meaning that the active Li in the cathode is no longer restored completely and that the Li reservoir in the anode is consumed. However, the additional Li amount introduced to the systems by pre-lithiation still leads to a significantly higher capacity in comparison to the full-cell using the pristine Si/C electrodes (Figure 7c and d). Comparing the different pre-lithiation techniques, the long-term cycling performance of the electrochemically pre-lithiated Si/C electrode at high specific currents, shows the lowest capacity retention.

For all full-cells, a potential shift to higher potentials was noticed for both negative and positive electrodes upon cycling, because of continuous active lithium losses due to SEI breakage and re-formation at the Si/C electrodes, see also Krueger *et al.*^[35] This electrode potential slippage is summarized in Figure 8, showing similar potential shifts for all setups between the 4th and 95th cycle. Overall, the pre-lithiated Si/C electrodes exhibit a lower potential due to the additional Li provided via pre-lithiation, which in turn results in improved cycle life.

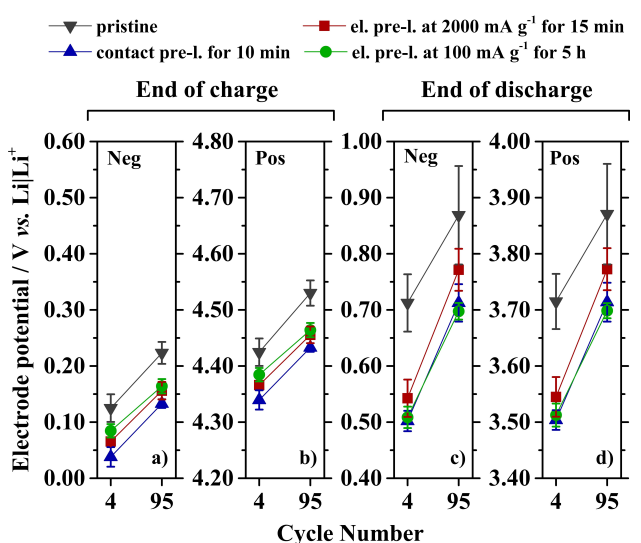


Figure 8. Si/C and NCM111 electrode potential shifts in NCM111 || Si/C cells (full-cell setup, three-electrode configuration) between the 4th and 95th cycle at the end of charge (a, b) and at the end of discharge (c, d). (a) and (c) show the negative electrode potential changes, while (b) and (d) show the positive electrode potential changes. The y-axis always has the same range (0.6 V) for better comparison of the shifts.

3. Conclusions

Within this work, we evaluated the impact of two different pre-lithiation approaches on the electrochemical performance and formation of the solid electrolyte interphase (SEI) of silicon/carbon (Si/C) negative electrodes. In particular, electrochemical pre-lithiation of Si/C electrodes at two different specific currents and pre-lithiation *via* direct contact to Li metal were analyzed with respect to the electrochemical performance in Si/C||Li metal half-cells and NCM111||Si/C full-cells. Further, the impact of the pre-lithiation approaches on SEI formation was thoroughly investigated *via* XPS.

Therefore, independent of the pre-lithiation technique, similar pre-lithiation degrees of the Si/C electrodes were reached, which was essential to enable a proper comparison between the different approaches. By pre-lithiation, the capacity retention of NCM111||Si/C full-cells was clearly improved. A huge percentage of active lithium losses in the first charge/discharge cycle was circumvented due to the SEI formed during pre-lithiation. Additionally, lithiation of the active material during pre-lithiation led to creation of a Li reservoir within the anode, which could buffer on-going Li consumption resulting in an increased Coulombic efficiency for over 40 cycles. Both effects reduced the depletion of the active Li from the positive electrode and, therefore, increased the capacity of the cell. The same electrode and cell setup as well as cycling procedures were used for all experiments, enabling a fair comparison between two pre-lithiation techniques. We were able to show that although there were minor differences in the composition of the SEI, pre-lithiation of the Si/C electrodes *via* both pre-lithiation methods enabled a quite similar improvement in terms of an improved electrochemical performance of NCM111||Si/C full-cells.

Various pre-lithiation approaches have been reported to compensate for active lithium losses of the initial charge/discharge cycle(s), such as chemical pre-lithiation by active reactants, use of lithiated active materials as anode additives, "contact pre-lithiation" by stabilized Li metal powder, etc. However, many of the approaches suffer from high reactivity, poor stability and/or high safety issues, changes of the production process (*e.g.*, use of different solvents or binders), or poor homogeneity of pre-lithiation. Therefore, only some of these approaches are potentially suitable for industrial manufacturing processes. The methods applied in this work are both *ex-situ* methods and are highly feasible in lab-scale, however, require dis- and reassembling of the cell after pre-lithiation, which is not a practical approach for large-scale manufacturing of pre-lithiated electrodes/cells. However, there are also approaches for roll-to-roll pre-lithiation methods, *i.e.*, electrochemical pre-lithiation with LiCl ("electrochemical bath") and pre-lithiation *via* short circuiting with Li metal. In particular, pre-lithiation by the "electrochemical bath" (electrolysis) approach seems to be one of the most promising strategies, *i.e.*, due to the avoidance of reactive salts, use of low-cost Li salts, and most likely a homogeneous pre-lithiation.^[9a,11a] As pre-lithiation is considered as additional manufacturing step during electrode/cell production, the overall pre-lithiation time should

be kept as short as possible. Future studies should therefore focus on further improving the pre-lithiation process (*e.g.*, short pre-lithiation times, use of effective SEI-forming electrolyte additives, *etc.*) and evaluate the impact of the respective approach on the long-term cycling performance in LIB full-cells.

Acknowledgements

We wish to thank the Federal Ministry for Economic Affairs and Energy (BMWi) for funding this work in the project "Go3" (03ETE002D). We also thank the Federal Ministry of Education and Research (BMBF) for funding this work in the project "PräLi" (03XP0238C) within the ProZell competence cluster. We thank Andre Bar for graphical support. Open access funding enabled and organized by Projekt DEAL.

Conflict of Interest

The authors declare no conflict of interest.

Keywords: pre-lithiation · silicon anode · Coulombic efficiency · active lithium loss · lithium-ion full-cell

- [1] M. Winter, B. Barnett, K. Xu, *Chem. Rev.* **2018**, *118*, 11433–11456.
- [2] a) D. Andre, H. Hain, P. Lamp, F. Maglia, B. Stiaszny, *J. Mater. Chem. A* **2017**, *5*, 17174–17198; b) G. E. Blomgren, *J. Electrochem. Soc.* **2017**, *164*, A5019–A5025; c) R. Schmuck, R. Wagner, G. Hörpel, T. Placke, M. Winter, *Nat. Energy* **2018**, *3*, 267–278; d) T. Placke, R. Kloepsch, S. Dühnen, M. Winter, *J. Solid State Electrochem.* **2017**, *21*, 1939–1964.
- [3] a) M. N. Obrovac, V. L. Chevrier, *Chem. Rev.* **2014**, *114*, 11444–11502; b) M. N. Obrovac, L. J. Krause, *J. Electrochem. Soc.* **2007**, *154*, A103–A108.
- [4] a) U. Kasavajjula, C. Wang, A. J. Appleby, *J. Power Sources* **2007**, *163*, 1003–1039; b) J. Yang, *Electrochem. Solid-State Lett.* **1999**, *2*, 161–163; c) C. K. Chan, H. Peng, G. Liu, K. McIlwrath, X. F. Zhang, R. A. Huggins, Y. Cui, *Nat. Nanotechnol.* **2008**, *3*, 31–35; d) M.-H. Park, M. G. Kim, J. Joo, K. Kim, J. Kim, S. Ahn, Y. Cui, J. Cho, *Nano Lett.* **2009**, *9*, 3844–3847; e) J. Müller, M. Abdollahifar, A. Vinograd, M. Nöske, C. Nowak, S.-J. Chang, T. Placke, W. Haselrieder, M. Winter, A. Kwade, N.-L. Wu, *Chem. Eng. J.* **2020**, 126603.
- [5] a) F. Holtstiege, A. Wilken, M. Winter, T. Placke, *Phys. Chem. Chem. Phys.* **2017**, *19*, 25905–25918; b) M. Ruttner, V. Siozios, M. Winter, T. Placke, *ACS Appl. Mater. Interfaces* **2020**, *3*, 743–758.
- [6] G. G. Eshetu, E. Figgemeier, *ChemSusChem* **2019**, *12*, 2515–2539.
- [7] a) J. R. Szczecz, S. Jin, *Energy Environ. Sci.* **2011**, *4*, 56–72; b) R. Nölle, K. Beltrup, F. Holtstiege, J. Kasnatscheew, T. Placke, M. Winter, *Mater. Today* **2020**, *32*, 131–146; c) A. J. Smith, J. C. Burns, D. Xiong, J. R. Dahn, *J. Electrochem. Soc.* **2011**, *158*, A1136–A1142; d) W. M. Dose, V. A. Maroni, M. J. Piernas-Muñoz, S. E. Trask, I. Bloom, C. S. Johnson, *J. Electrochem. Soc.* **2018**, *165*, A2389–A2396.
- [8] a) F. Holtstiege, P. Bärmann, R. Nölle, M. Winter, T. Placke, *Batteries* **2018**, *4*, 4; b) V. Aravindan, Y.-S. Lee, S. Madhavi, *Adv. Energy Mater.* **2017**, *7*, 1602607; c) K. Zou, W. Deng, P. Cai, X. Deng, B. Wang, C. Liu, J. Li, H. Hou, G. Zou, X. Ji, *Adv. Funct. Mater.* **2020**, *10*, 2005581.
- [9] a) V. L. Chevrier, L. Liu, R. Wohl, A. Chandrasoma, J. A. Vega, K. W. Eberman, P. Stegmaier, E. Figgemeier, *J. Electrochem. Soc.* **2018**, *165*, A1129–A1136; b) M.-T. F. Rodrigues, J. A. Gilbert, K. Kalaga, D. P. Abraham, *J. Phys.: Energy* **2020**, *2*, 24002.
- [10] a) M. Klett, J. A. Gilbert, S. E. Trask, B. J. Polzin, A. N. Jansen, D. W. Dees, D. P. Abraham, *J. Electrochem. Soc.* **2016**, *163*, A875–A887; b) N. Delpuech, N. Dupre, P. Moreau, J.-S. Bridel, J. Gaubicher, B. Lestriez, D. Guyomard, *ChemSusChem* **2016**, *9*, 841–848; c) N. Dupré, P. Moreau, E.

- de Vito, L. Quazuguel, M. Boniface, A. Bordes, C. Rudisch, P. Bayle-Guillemaud, D. Guyomard, *Chem. Mater.* **2016**, *28*, 2557–2572.
- [11] a) H. J. Kim, S. Choi, S. J. Lee, M. W. Seo, J. G. Lee, E. Deniz, Y. J. Lee, E. K. Kim, J. W. Choi, *Nano Lett.* **2016**, *16*, 282–288; b) M. W. Forney, M. J. Ganter, J. W. Staub, R. D. Ridgley, B. J. Landi, *Nano Lett.* **2013**, *13*, 4158–4163; c) N. Liu, L. Hu, M. T. McDowell, A. Jackson, Y. Cui, *ACS Nano* **2011**, *5*, 6487–6493; d) A. Shellikeri, V. G. Watson, D. L. Adams, E. E. Kalu, J. A. Read, T. R. Jow, J. P. Zheng, *ECS Trans.* **2017**, *77*, 293–303; e) B. B. Fitch, M. Yakovleva, Y. Li, I. Plitz, A. Skrzypczak, F. Badway, G. G. Amatucci, Y. Gao, *ECS Trans.* **2007**, *3*, 15–22; f) F. Holtstiege, R. Schmuck, M. Winter, G. Brunklaus, T. Placke, *J. Power Sources* **2018**, *378*, 522–526; g) P. Bärmann, M. Diehl, L. Göbel, M. Ruttert, S. Nowak, M. Winter, T. Placke, *J. Power Sources* **2020**, *464*, 228224.
- [12] M. Saito, K. Kato, S. Ishii, K. Yoshii, M. Shikano, H. Sakaebe, H. Kiuchi, T. Fukunaga, E. Matsubara, *J. Electrochem. Soc.* **2019**, *166*, A5174–A5183.
- [13] Y. Arinicheva, M. Wolff, S. Lobe, C. Dellen, D. Fattakhova-Rohlfing, O. Guillou, D. Böhm, F. Zoller, R. Schmuck, J. Li, M. Winter, E. Adamczyk, V. Pralong in *Advanced Ceramics for Energy Conversion and Storage*, Elsevier, **2020**, pp. 549–709.
- [14] a) K. Kinoshita, K. Zaghib, *J. Power Sources* **2002**, *110*, 416–423; b) P. Meister, H. Jia, J. Li, R. Kloepsch, M. Winter, T. Placke, *Chem. Mater.* **2016**, *28*, 7203–7217.
- [15] a) H. Bryngelsson, M. Stjerndahl, T. Gustafsson, K. Edström, *J. Power Sources* **2007**, *174*, 970–975; b) K. Edström, M. Herstedt, D. P. Abraham, *J. Power Sources* **2006**, *153*, 380–384; c) K. Xu, *Chem. Rev.* **2004**, *104*, 4303–4418.
- [16] B. Key, R. Bhattacharyya, M. Morcrette, V. Seznec, J.-M. Tarascon, C. P. Grey, *J. Am. Chem. Soc.* **2009**, *131*, 9239–9249.
- [17] P. Bärmann, B. Krueger, S. Casino, M. Winter, T. Placke, G. Wittstock, *ACS Appl. Mater. Interfaces* **2020**, *12*, 55903–55912.
- [18] K. Kalaga, M.-T. F. Rodrigues, S. E. Trask, I. A. Shkrob, D. P. Abraham, *Electrochim. Acta* **2018**, *280*, 221–228.
- [19] F. Holtstiege, T. Koç, T. Hundhege, V. Siozios, M. Winter, T. Placke, *ACS Appl. Mater. Interfaces* **2018**, *1*, 4321–4331.
- [20] M. N. Obrovac, L. Christensen, *Electrochim. Solid-State Lett.* **2004**, *7*, A93–A96.
- [21] a) S. A. Delp, O. Borodin, M. Olguin, C. G. Eisner, J. L. Allen, T. R. Jow, *Electrochim. Acta* **2016**, *209*, 498–510; b) P. Verma, P. Maire, P. Novák, *Electrochim. Acta* **2010**, *55*, 6332–6341; c) C. K. Chan, R. Ruffo, S. S. Hong, Y. Cui, *J. Power Sources* **2009**, *189*, 1132–1140.
- [22] a) C. Shen, R. Fu, Y. Xia, Z. Liu, *RSC Adv.* **2018**, *8*, 14473–14478; b) R. Nölle, J.-P. Schmiegel, M. Winter, T. Placke, *Chem. Mater.* **2020**, *32*, 173–185.
- [23] C. C. Nguyen, B. L. Lucht, *J. Electrochem. Soc.* **2014**, *161*, A1933–A1938.
- [24] a) N.-S. Choi, K. H. Yew, K. Y. Lee, M. Sung, H. Kim, S.-S. Kim, *J. Power Sources* **2006**, *161*, 1254–1259; b) C. C. Nguyen, T. Yoon, D. M. Seo, P. Guduru, B. L. Lucht, *ACS Appl. Mater. Interfaces* **2016**, *8*, 12211–12220.
- [25] a) R. Nölle, A. J. Achazi, P. Kaghazchi, M. Winter, T. Placke, *ACS Appl. Mater. Interfaces* **2018**, *10*, 28187–28198; b) R. Dedryvère, L. Gireaud, S. Grangeon, S. Laruelle, J.-M. Tarascon, D. Gonbeau, *J. Phys. Chem. B* **2005**, *109*, 15868–15875; c) A. L. Michan, B. S. Parimalam, M. Leskes, R. N. Kerber, T. Yoon, C. P. Grey, B. L. Lucht, *Chem. Mater.* **2016**, *28*, 8149–8159.
- [26] B. Philippe, R. Dedryvère, J. Allouche, F. Lindgren, M. Gorgoi, H. Rensmo, D. Gonbeau, K. Edström, *Chem. Mater.* **2012**, *24*, 1107–1115.
- [27] T. Jaumann, J. Balach, M. Klose, S. Oswald, U. Langklotz, A. Michaelis, J. Eckert, L. Giebel, *Phys. Chem. Chem. Phys.* **2015**, *17*, 24956–24967.
- [28] E. Radvanyi, E. de Vito, W. Porcher, S. Jouanneau Si Larbi, *J. Anal. At. Spectrom.* **2014**, *29*, 1120–1131.
- [29] K. W. Schroder, H. Celio, L. J. Webb, K. J. Stevenson, *J. Phys. Chem. C* **2012**, *116*, 19737–19747.
- [30] D. D. Ma, C. S. Lee, F. C. K. Au, S. Y. Tong, S. T. Lee, *Science* **2003**, *299*, 1874–1877.
- [31] M. Nie, D. P. Abraham, Y. Chen, A. Bose, B. L. Lucht, *J. Phys. Chem. C* **2013**, *117*, 13403–13412.
- [32] a) F. Reuter, A. Baasner, J. Pampel, M. Piwko, S. Dörfler, H. Althues, S. Kaskel, *J. Electrochem. Soc.* **2019**, *166*, A3265–A3271; b) J. Kasnatscheew, T. Placke, B. Streipert, S. Rothermel, R. Wagner, P. Meister, I. C. Laskovic, M. Winter, *J. Electrochem. Soc.* **2017**, *164*, A2479–A2486.
- [33] a) J. Kasnatscheew, M. Evertz, B. Streipert, R. Wagner, R. Klöpsch, B. Vortmann, H. Hahn, S. Nowak, M. Amereller, A.-C. Gentschev, P. Lamp, M. Winter, *Phys. Chem. Chem. Phys.* **2016**, *18*, 3956–3965; b) S.-H. Kang, W.-S. Yoon, K.-W. Nam, X.-Q. Yang, D. P. Abraham, *J. Mater. Sci.* **2008**, *43*, 4701–4706; c) X. Zhang, W. J. Jiang, A. Mauger, Qiliu, F. Gendron, C. M. Julien, *J. Power Sources* **2010**, *195*, 1292–1301.
- [34] a) I. Buchberger, S. Seidlmayer, A. Pokharel, M. Piana, J. Hattendorff, P. Kudejova, R. Gilles, H. A. Gasteiger, *J. Electrochem. Soc.* **2015**, *162*, A2737–A2746; b) J. Kasnatscheew, U. Rodehorst, B. Streipert, S. Wiemers-Meyer, R. Jakelski, R. Wagner, I. C. Laskovic, M. Winter, *J. Electrochem. Soc.* **2016**, *163*, A2943–A2950.
- [35] S. Krueger, R. Kloepsch, J. Li, S. Nowak, S. Passerini, M. Winter, *J. Electrochem. Soc.* **2013**, *160*, A542–A548.

Manuscript received: January 27, 2021

Revised manuscript received: March 3, 2021

Accepted manuscript online: March 17, 2021

Version of record online: March 30, 2021